Saleem H. Trier

Department of Medical Physics, College of Science, University of Al- Qadisiyah, Diwaniyah, IRAQ

Study of Optical, Electrical, and Structural Properties of Zinc-Doped CdTe Films by Chemical Bath Deposition

Thin layer coatings of CdZnTe were prepared using a non-aqueous chemical bath deposition method. X-ray diffraction (XRD), scanning electron microscopy (SEM), field-emission scanning electron microscopy (FE-SEM), Fourier-transform infrared spectroscopy (FTIR), photoluminescence (PL), UV-visible spectroscopy, Raman spectroscopy, and Hall effect analysis were used to examine the deposited films. Results indicates that the deposited films exhibit polycrystalline characteristics of cubic zinc-blende. Evaluations were conducted on the structural characteristics, including dislocation density, lattice constant, micro-strain, and crystallite size. The as deposited films are smooth, uniformly sized, spherical grains that are dispersed in both single-state and cluster form, according to FE-SEM and SEM results. It was found that the average crystallite size of the film was 12.33 nm and the energy gap was 2.2 eV, which is responsible for the large transmittance, and that the resistivity of the film deposited at room temperature was 5×10^3 Ω.m.

Keywords: CdZnTe; Thin films; Chemical bath deposition, Structural characteristics
Received: 04 November; **Revised:** 05 December; **Accepted:** 12 December 2023

1. Introduction

CdZnTe is a direct energy gap semiconductor with outstanding properties and is from the most suitable materials for ambient temperature detectors for X-rays and gamma rays due to its short leakage currents as well as high quantum efficiency in detector sensors [1]. CdZnTe is an interesting subject for imparting exotic electrical and optical properties. CdZnTe has a triplet energy gap which is constant for all alloy compounds and can be estimated at approximately (1.5-2.3) eV at ambient temperature [2]. It has been shown that several physical features are required to operate the detector, for example increased atomic number (2) to achieve the good atomic radioactive conductivity, and a sufficiently large energy gap is required. To achieve a high magnitude resistivity to keep the noise associated with the short external flux current in the sensor. The broad cross-sectional area of photoelectric absorption of gamma rays allows for efficient conversion of gamma ray energy into electrical energy, a large intrinsic mobility lifetime (μτ) product, and a reduction in electronic interference. The cubic zinc hybrid lattice of this ternary compound has an atomic number that is extremely similar to that of CdTe. CdZnTe has been applied to solid-state devices such solar cells, photodetectors or sensors, and light-emitting diodes [3]. The application of CdZnTe technology has expanded in recent years, particularly in the domains of space science, nuclear medicine, and national security. It is related to imaging techniques like x-ray or gamma-ray tomography, x-ray fluorescence, etc. in the field of nuclear medicine. Implementing national security mostly entails finding, following, or detecting radioactive elements. Examples of this include tracking nuclear power plants for environmental change and welfare, as well as inspecting nuclear weapons. The high energy focusing telescope is connected to implementation in space science (HEFT) [2]. Recently, a range of thin film deposition techniques, including as electrodeposition[4,5], thermal evaporation [6], magnetron sputtering [7], closed space sublimation [8], and chemical bath deposition [9], have been developed to create CdZnTe thin film layers.

Chemical bath deposition (CBD) technology is the most straightforward and cost-effective of all operating techniques. In comparison to other methods, it also offers vast area deposition and high deposition rates [10,11]. As a result, it satisfies the standards for the production of solar devices [9]. Since the non-aqueous mode allows greater flexibility and is more convenient than the aqueous mode, so in this study, CdZnTe films deposited on nickel substrates were prepared using chemical bath deposition in a non-aqueous medium. Working at high temperatures can be done using non-aqueous techniques, giving a wide range of substrates. Of course, no hydrogen gas is produced, unlike the water-based concept, leaving a hole-free layer. Detectable and post-infrared optical transmission, X-ray diffraction, and field emission scanning electron microscopy (FE-SEM) were used to analyze the deposited layers.

2. Experimental Techniques

0.05M TeO_2, 0.05M cadmium acetate ($Cd(CH_3CO_2)$), 0.125M $NaBH_4$, and 0.5M $ZnCl_2$ deliquesced in 40ml ethylene glycol were used to aggregate the osmolality. First, fill a beaker with 40 mol of ethylene glycol. Stir the mixture moderately for two hours using a magnetic stirrer, and maintain the temperature of the combined solution at 160°C. 0.05M TeO_2 is added and stirred for 10min., followed

by 0.05M Cadmium acetate and 5min. of stirring. After the compound reaches 160°C, 0.125M $NaBH_4$ is added and stirred for 2hours ,Finally, 0.5 M ZnC_{l2} was introduced into the solution and stirred for the next 2 hours. With the help of a rigid support, a Ni plate of size 2.5×1.5cm was immersed in the electrolyte and the film was continuously deposited for 15min.

The color of the sediment is black. The films were washed with distilled water and dried at room temperature. Examine the structural form and composition as well as optical properties of the deposited film to observe its solid-state properties.

3 .Results and Discussion

Figure (1) displays the x-ray diffraction pattern of the CdZnTe film that was deposited on a Ni substrate. The final film has good physical stability and adhesion. The range of the XRD spectra is still (20-90)°. The figure illustrates the indicated peaks present in the CdZnTe film at 2θ = 23.01°, 40.45°, 51.27°, 56.9°, 67.7°, and 81.4°. These peaks are recognized as (111), (220), diffraction planes of (222), (400), (331), (420), and (511) cubic zinc whisk structures [12]. It was discovered that the sphalerite structure's cubic phase with thin CdZnTe coatings was a feasible polycrystalline phase with a (111) preferred orientation [8]. Additionally, phase exclusion, or two aspects (ZnTe and CdTe) with ZnTe having (012) preferred orientation and CdTe having (222) and (331) preferred orientations, was detected in the deposited CdZnTe films. It displays, among other things, peaks for Cd and Te, where the optimal orientations for Cd are (101) and (110) and Te is (220). Scherrer's formula was used to get the average crystallite size (D), as indicated in Eq. (1) [13,14]. While the 2θ value of the (111) peak and the Bragg equation of the cubic arrangement both of which are given in table (1) are used to compute the lattice constant (a) and inter-planar spacing (d_{hkl}) of the cubic state.

$$D = \frac{K\lambda}{\beta\cos\theta} \quad (1)$$

To estimate the micro-strain in the film, use the following equation [15]

$$\epsilon = \frac{\beta\cos\theta}{4} \quad (2)$$

The deposited CdZnTe has an average particle size of about 68 nm. The cast film's CdZnTe lattice invariance coefficient is 6.7Å. It is well known that atoms' elimination discrepancies with respect to their reference lattice positions can alter the lattice tension in thin coatings that have been applied [8]. The dislocation density of the CdZnTe film that was deposited was determined by applying the Williamson-Smallman formula.

$$\sigma = \frac{1}{D^2} \quad (3)$$

The calculated 2θ, d_{hkl}, and Miller indices for the deposited CdZnTe thin film are provided in table (2). Table (3) lists dislocation density and the micro-strain of the CdZnTe thin films that were deposited.

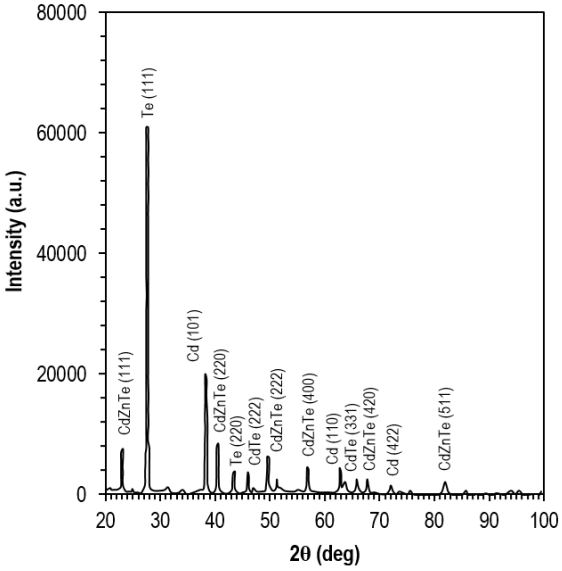

Fig. (1) XRD spectrum of the prepared CdZnTe thin film

Table (1) The inter-planer spacing (ISP), lattice constant (a), and crystalline size (D) of the deposited CdZnTe thin film

Sample	$d_{(hkl)}$ (Å)	Lattice Constant (a) (Å)	Average Crystalline Size (D) (nm)
1	3.854	6.692	67.87

Table (2) Values of 2θ, d_{hkl} , and Miller indices of the deposited CdZnTe thin film

Measured values			Standard values		
2θ (deg)	d_{hkl}	Miller indices	2θ (deg)	d_{hkl}	Miller indices
23.10	3.840	(111)	23.74	3.743	(111)
40.55	2.207	(220)	40.60	2.218	(220)
51.37	1.760	(222)	50.50	1.805	(222)
56.98	1.600	(400)	56.83	1.618	(400)
67.80	1.362	(420)	66.83	1.398	(420)
81.50	1.160	(511)	80.91	1.197	(511)

Table (3) Micro-strain and dislocation density of the CdZnTe thin film that were deposited

Micro-strain ($\times10^{-3}$)	Dislocation density ($\times10^{10}cm^{-2}$)
29.39	2.163

Surface diagnostics of deposited CdZnTe films using FESEM and SEM are displayed in Fig. (2). 25kX and 50kX magnifications were used for FE-SEM and SEM photography, respectively. The deposited layer shows smooth, consistently sized spherical particles, as the figure illustrates. The spherical particles are dispersed both single states and in clusters on the whole upper surface of the films. This demonstrates the CdZnTe film's crystallite nature. Agglomeration of CdZnTe elemental particles was seen in the FE-SEM and SEM of the formed films, leading to the formation of nanoclusters [16]. The film comparison also shows that the deposited

film contains thick grains with an average grain size of 12.33 nm and no holes or pits.

Figure (3) shows how the elements composition of the as-cast CdZnTe the film is analyzed. EDS signals were captured between 0 and 20 keV in binding energies. The as-deposited CdZnTe film contains zinc (Zn), tellurium (Te), and cadmium (Cd), as seen by the peaks in Fig. (3).

Table (4) shows the percentage weight and atomic content of the deposited film. It was found that the average atomic percentages of Cd, Zn, and Te were 17.64%, 1.44%, and 80.92%, respectively. As stated in the research [17], zinc's share of the element ratio in the CdZnTe film is significantly less than that of tellurium and cadmium. The deposition of stoichiometric films was revealed by EDS analysis of the as-deposited CdZnTe films.

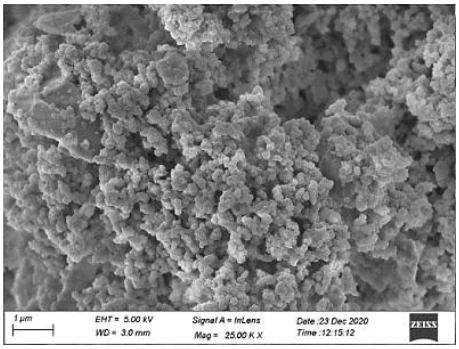

(1)

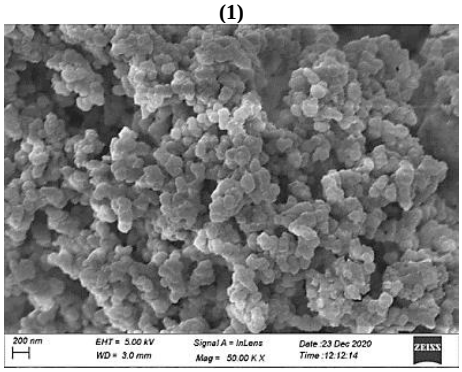

(2)

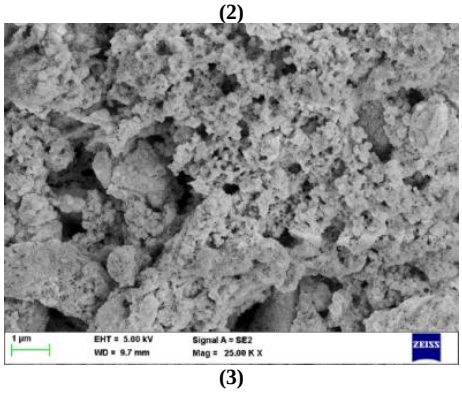

(3)

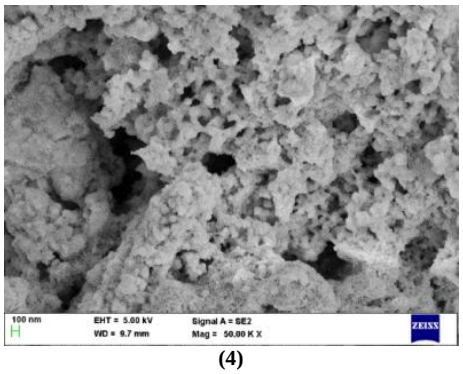

(4)

Fig. (2) FE-SEM and SEM images of the deposited CdZnTe film (1,2) FE-SEM at 25 and 50kX, (3,4) SEM at 25 and 50kX

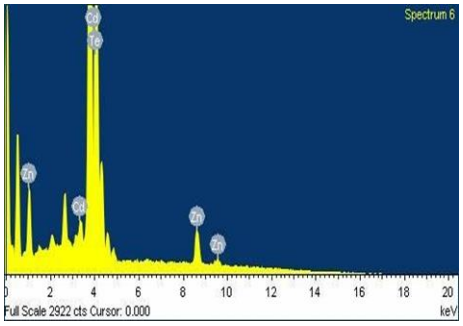

Fig. (3) EDS spectrum of the deposited CdZnTe film

Table (4) Elemental analysis of the deposited CdZnTe film

Element	Atomic (%)	Weight (%)
Cd	17.64	9.91
Zn	1.44	1.39
Te	80.29	88.71

The FTIR spectrum of the CdZnTe film as prepared is shown in Fig. (4). The CdZnTe sample demonstrates the existence of C-H, carboxyl, and hydroxyl groups. It also exhibits C-O stretching. The presence of OH stretching as a result of air pressure is shown by the large peak 3278.99 cm^{-1} [18]. The alkane functional group's C-H bent bond structure is thought to be represented by the tiny peak 1330.88 cm^{-1} [19]. Alkene (=C-H) bending vibration is present as indicated by the peak 921.97 cm^{-1} [20]. The stretching mode of aliphatic amines was identified as the peak 1072.42 cm^{-1} [21]. It is believed that the bending mode of aromatic C-H functional groups is responsible for the peak 682.80 cm^{-1} [22]. The appearing absorption band is associated with wave 856.39 cm^{-1} and can be ascribed to the CdZnTe thin-layer coating's stretching vibration [8]. Table (5) displays various functional groups found in the deposited CdZnTe films.

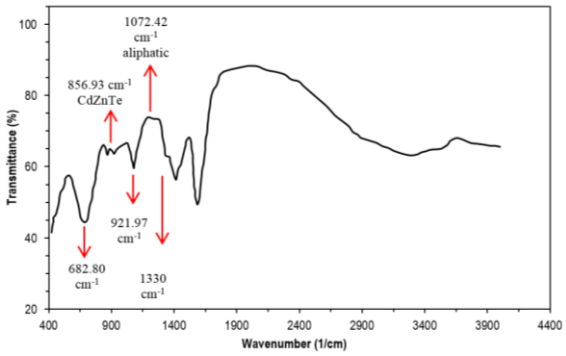

Fig. (4) FTIR spectrum of the deposited CdZnTe film

Table (5) Assignments of molecular vibrations of deposited CdZnTe film

Positions(cm^{-1})	Assignments
3278.99	O-H
1330.88	C-H
921.97	=C-H
1072.42	Aliphatic amines
682.80	C-H
856.39	CdZnTe

At room temperature, the optical absorption spectrum of the deposited CdZnTe thin film was recorded in the spectral range 200-800nm. The energy gap of CdZnTe film may be determined using the Tauc equation $(\alpha h\upsilon)^2=A(h\upsilon-E_g)^{1/2}$, which confirms that the material is a direct energy gap semiconductor [6]. In this equation, the absorption coefficient is α, the band gap is E_g, the frequency is υ, the proportionality constant is A, and the Planck's constant is h

Plotting $(\alpha h\upsilon)^2$ versus energy (hυ) and energy gap (E_g) of deposited CdZnTe thin film, as seen by extrapolating the curve of $(\alpha h\upsilon)^2=0$, illustrates the optical absorption extension of a CdZnTe film in Fig. (5). It was discovered that the as-deposited CdZnTe film had an energy band width of 2.2eV. The outcomes agree with the published research [8,23,24]. The Tauc plot's roughly linear behavior suggests that CdZnTe is a direct energy gap semiconductor.

It has been stated that there is a greater energy gap between pure and doped CdTe nanocrystals. The two primary causes of an increase in band gap are (1) alloying with materials that have a greater band gap, and (2) quantum confinement of energy levels within nanocrystals [25].

The photoluminescence spectrum of deposited CdZnTe is depicted in Fig. (6). The non-destructive photoluminescence (PL) spectroscopy is frequently used to investigate the inherent and external characteristics of bulk semiconductors and nanostructures. This PL intensity and spectral content provide precise measures of a range of superior material characteristics. This method uses laser light with accompanying energy far bigger than the optical band gap to produce excitation. It is clear that the deposited CdZnTe film has a broad emission spectrum at 448 and 469 nm, respectively, and a fluorescence peak at 374 nm as shown in Fig. (6). The particle size dispersion of CdZnTe nanocrystal films is the cause of this widespread emission [26-28].

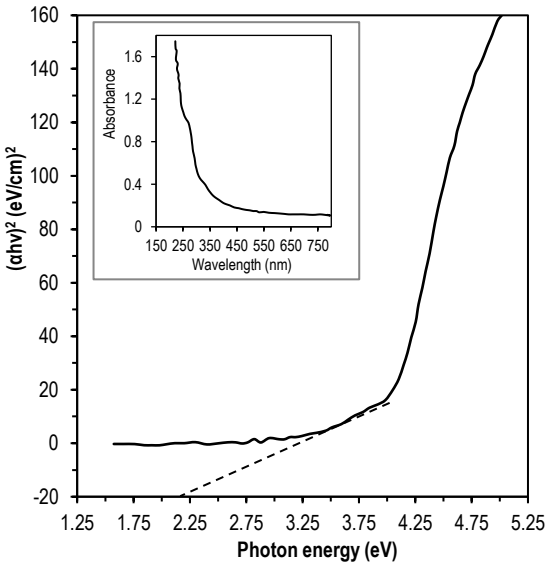

Fig. (5) Determination of energy gap and absorbance of the deposited CdZnTe film

The spectrum also shows that the bulk CdZnTe crystals are responsible for the higher wavelengths, whereas the lesser wavelengths are related to the smaller size of CdZnTe quantum dots. A widening of the emission peak at 469 nm, an indication of CdZnTe nanocrystalline layer formation and deep trap emission, was seen when Zn was doped with CdTe films [29].

An additional practical technique for identifying material phases and assessing the crystallinity of films is Raman spectroscopy. This method uses the inelastic scattering of monochromatic photons to monitor vibrations, rotations, and other low-frequency modes in molecules. Transverse optics (TO) and longitudinal optics (LO) of deposited phonon mode CdTe were stated in Ref. [30] as well as a clear peak of Raman at 166, 139 and 332 cm^{-1} in the Raman spectra produced for the sample using a wavelength of 785 nm, an exposure duration of 10 s, and a power of 0.1 mW. Common Te inclusions in crystalline CdTe have been effectively detected using Raman spectroscopy. There is a difference between the Raman longitudinal optics of the LO mode of crystalline CdTe and the A1 mode of crystalline tellurium. For these reasons, x-ray techniques may not always be able to see Te inclusions in CdTe that are discovered by Raman scattering. Crystalline materials' Raman spectrum can only display modes where ω deviates from zero at $q \approx 0$. An amorphous material's Raman spectrum is frequency dependent and typically broadens to match its whole vibrational dynamic density (DOS). The term "modulation" refers to the local atomic environment's symmetry. This is because, in theory, all Raman and infrared

vibration modes become active when the momentum conservation selection criteria for Raman scattering is applied to the amorphous state [31].

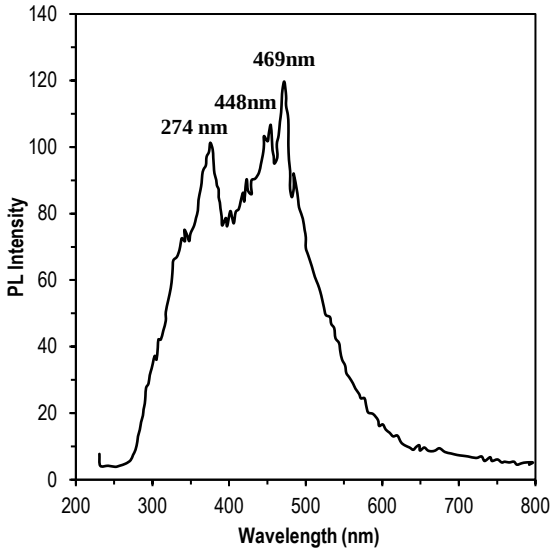

Fig. (6) PL spectrum of the deposited CdZnTe film

Other semiconductors have been subjected to this study. The peak characteristics of CdTe are shown in Fig. (7), where A1 is represented by the first peak seen at 119 cm^{-1}, the second at 139 cm^{-1}, the third at 166 cm^{-1}, and the fourth at 332 cm^{-1} (LO). The longitudinal optical phonon vibration mode (LO) of Te and the transverse optical phonon vibration mode (2LO) of CdTe are the corresponding E modes. It is noteworthy that Te/Raman modes are frequently found in CdTe samples, which may be the result of trace amounts of Te precipitates [32,33].

CdZnTe film resistivity was calculated using Hall effect technique. Equation (4) is used to compute resistivity (ρ).

$$\rho = \frac{V}{I} \times 2\pi S \qquad (4)$$

where I is the current flowing into and out of the outer probe, V is the potential difference between the inner probes, and S is the probe distance (0.2cm). The temperature range in which CdZnTe resistivity is estimated is 303-363K. It was discovered that the resistivity of CdZnTe at room temperature was 5×10^3 Ω.m. Resistivity for semiconductors diminishes with temperature. The resistivity of CdZnTe as deposited is displayed in Fig. (8). The figure illustrates how resistivity falls with temperature because excited electrons in the valence band hop to the conduction band, increasing conductance and resulting in a decrease in resistivity. Resistivity will likewise decrease since resistance is proportionate to resistivity [34,35]. The plot of $\log_{10}\rho$ versus 1/T yields a linear curve at higher temperatures. As a result, the width of the energy gap can be estimated from the slope of the linear section of the experimental curve.

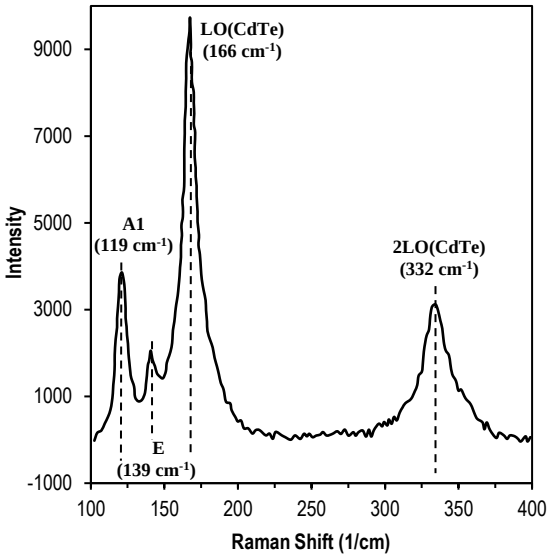

Fig. (7) Raman spectrum of the deposited CdZnTe film

The formula for calculating the energy gap is $E_g=2.3\times2k_B\Delta\log_{10}\rho/\Delta T^{-1}$, where k_B is Boltzmann's constant. The band gap was discovered to be 1.98 eV, which agrees with the band gap determined using reported work and Tauc's formula (band gap variation is roughly 1.4-2.2eV) [8,23,24].

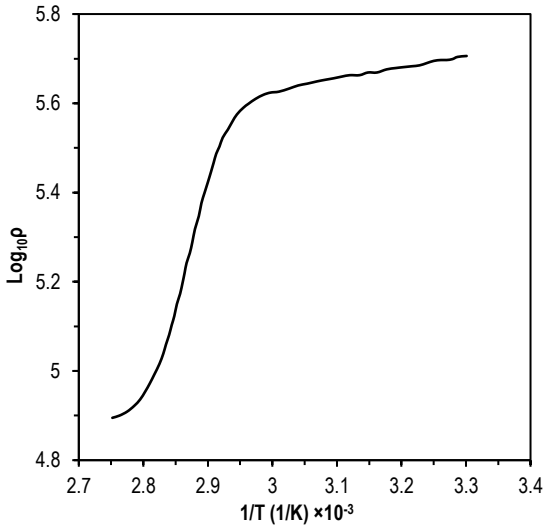

Fig. (8) Variation of $\log_{10}\rho$ with reciprocal temperature (1/T) for the deposited CdZnTe films

4. Conclusion

A non-aqueous mode chemical bath deposition approach was used to easily produce cubic zinc stirred CdZnTe films on Ni substrates. Using various methods, the solid-state and as well as optical characteristics of deposited CdZnTe films were investigated. Cubic zincblende phase of CdZnTe was confirmed. The surface is uniform, dense, and devoid of voids. With some Te still present, the deposited film's stoichiometry is precisely observed. Based on the light absorption extension, a pre-designed band gap of 2.2eV was assigned. CdZnTe has a resistivity of 5×10^3 Ω.m. Photoluminescence reveals emission

from deep traps. The LO and 2LO modes of CdTe phonon vibration were observed at 166 and 332cm^{-1}, respectively, according to Raman analysis. These features make CdZnTe films suitable for use in sensor, photovoltaic, and photoelectrochemical cells.

References

[1] N. Manez et al., "Material optimization for X-ray imaging detectors", *Nucl. Instrum. Methods Phys. Res. A*, 567(1) (2006) 281-284.

[2] S. Jain, "Photoluminescence study of cadmium zinc telluride", MSc thesis, West Virginia University (USA, 2001).

[3] S.D. Sordo et al., "Progress in the Development of CdTe and CdZnTe Semiconductor Radiation Detectors for Astrophysical and Medical Applications", *Sensors*, 9(5) (2009) 3491-3526.

[4] K.R. Murali et al., "Properties of CdTe films deposited by electron beam evaporation", *Surf. Coat. Technol.*, 41(2) (1990) 211-219.

[5] A. Bansal and P. Rajaram, "Electrochemical growth of CdZnTe thin films", *Mater. Lett.*, 59(28) (2005) 3666-3671.

[6] G. Zha et al., "The growth and the interfacial layer of CdZnTe nano-crystalline films by vacuum evaporation", *Vacuum*, 86(3) (2011) 242-245.

[7] P. Banerjee, R. Ganguly and B. Ghosh, "Optical properties of $Cd_{1-x}Zn_xTe$ thin films fabricated through sputtering of compound semiconductors", *Appl. Surf. Sci.*, 256(1) (2009) 213-216.

[8] H. Xu et al., *Appl. Surf. Sci.*, "The dependence of Zn content on thermal treatments for $Cd_{1-x}Zn_xTe$ thin films deposited by close-spaced sublimation" 305 (2014) 477-480.

[9] T. Yamaguchi et al., "Preparation and characterization of (Cd,Zn)S thin films by chemical bath deposition for photovoltaic devices", *Thin Solid Films*, 343-344 (1999) 516-519.

[10] J. Zhou et al., "CBD-$Cd_{1-x}Zn_xS$ thin films and their application in CdTe solar cells", *phys. stat. sol. (b)*, 241(3) (2004) 775-778.

[11] N. Gaewdang and T. Gaewdang, "Investigations on chemically deposited $Cd_{1-x}Zn_xS$ thin films with low Zn content" *Mater. Lett.*, 59(28) (2005) 3577-3584.

[12] S. Chander and M.S. Dhaka, "Thermal annealing induced physical properties of electron beam vacuum evaporated CdZnTe thin films", *Thin Solid Films*, 625 (2017) 131-137.

[13] S. Chander and M.S. Dhaka, "Effect of thickness on physical properties of electron beam vacuum evaporated CdZnTe thin films for tandem solar cells" *Physica E: Low-Dim. Sys. Nanostruct.*, 84 (2016) 112-117.

[14] S.H. Trier, "The Study of $Mg_{1-x}Co_xFe_2O_4$ Ferrite Physical Properties and its Applications", *NeuroQuantology*, 18(2) (2020) 143-156.

[15] M.K. Ashok and S. Muthukumaran, Phys. Proced., 49 (2013) 137-???.

[16] G. Rajesh et al., "Photoinduced electrical bistability of sputter deposited CdZnTe thin films", *Mater. Res. Exp.*, 5 (2018) 026412.

[17] S. Chander and M.S. Dhaka, "Optimization of structural, optical and electrical properties of CdZnTe thin films with the application of thermal treatment", *Mater. Lett.*, 182 (2016) 98-101.

[18] S. R. Kumar et al., "Structure, Composition and Optical Properties of Non Aqueous Deposited ZnCdS Nanocrystalline Film", *Mater. Today: Proc.*, 2(9A) (2015) 4563-4568.

[19] M.K. Bin Bakri and E. Jayamani, **"Science, Humanities, and Technology"**, 1st ed., Tro India (2016) Ch. 30, p. 167.

[20] E. Al-Shareefi, A.H. Abdual Sahib and I.H. Hameed, *Indian J. Public Health Res. Develop.*, 10(1) (2019) 994.

[21] N. Janakiraman and M. Johnson, "Functional Groups of Tree Ferns (Cyathea) Using FT-IR: Chemotaxonomic Implications", *Romanian J. Biophys.*, 25(2) (2015) 131-141.

[22] K. Banerjee, N. Thiagarajan and P. Thiagarajan, "Azadirachta indica A. Juss Based Emollient Cream for Potential Dermatological Applications", *Indian J. Pharmaceut. Sci.*, 78(3) (2016) 320-325.

[23] E. Yilmaz, "An Investigation of CdZnTe Thin Films for Photovoltaics", *Ener. Sour. A*, 34(4) (2011) 332-335

[24] M. Dammak et al., "Optical spectroscopy of titanium-doped CdZnTe", *Semicond. Sci. Technol.*, 13(7) (1998) 762-768.

[25] A. Al-Rasheedi et al., "Structural and optical properties of CdZnTe quantum dots capped with a bifunctional Molecule", J. Mater. Sci.: Mater. Electron., 28(12) (2017) 9114.

[26] A. Khare, "Effects of the Zn concentration on electro-optical properties of $Zn_xCd_{1-x}S$ films", *Chalcogen. Lett.*, 6(12) (2009) 661-671.

[27] M.A. Mahdi et al., "Structural and optical properties of nanocrystalline CdS thin films prepared using microwave-assisted chemical bath deposition", *Thin Solid Films*, 520(9) (2012) 3477-3484.

[28] C.S. Tiwary et al., "Synthesis of wurtzite-phase ZnS nanocrystal and its optical properties", *J. Lumines.*, 129(11) (2009) 1366-1370.

[29] C. Jin et al., "Synthesis and Wavelength-Tunable Luminescence Property of Wurtzite $Zn_xCd_{1-x}S$ Nanostructures", *Cryst. Growth Des.*, 9(11) (2009) 4602-4606.

[30] H. Park et al., "CdTe microwire-based ultraviolet photodetectors aligned by a non-uniform electric field ", *Appl. Phys. Lett.*, 103 (2013) 051906.

[31] Z. Bai and D. Wang, "Oxidation of CdTe thin film in air coated with and without a CdCl2 layer", *phys. stat. sol. (a)*, 209(10) (2012) 1982-1987.

[32] E. Campos-González et al., "Structural and optical properties of CdTe-nanocrystals thin films grown by chemical synthesis", *Mater. Sci. Semicond. Process.*, 35 (2015) 144-148.

[33] Y. Xu et al., "Study on temperature dependent resistivity of indium-doped cadmium zinc telluride", *J. Phys. D: Appl. Phys.*, 42(3) (2009) 035105.

[34] S. Rajpal and S.R. Kumar, "Annealing temperature dependent structural and optical properties of nanocrystalline ZnTe thin films developed by electrodeposition technique", *Solid State Sci.*, 108 (2020) 106424.

[35] G. Morell, A. Reynes-Figueroa and R.S. Katiyar, "Raman spectroscopy of oxygenated amorphous CdTe films", *J. Raman Spectro.*, 25(3) (1994) 203-207.

